International Journal of
Metallurgical & Materials Engineering
Research Article Open Access

Reciprocating Wear Behavior of Al Alloys: Effect of Porosity and Normal Load

Avijit Sinha, Md. Aminul Islam* and Zoheir Farhat
Department of Process Engineering and Applied Science, Materials Engineering Program, Dalhousie University, Halifax, Nova Scotia, B3J2X4, Canada

Abstract

Aluminum alloys are attractive for critical applications such as pistons, clutch housings and liners in automotive industry for their high strength to weight ratio, high corrosion resistance and good heat conductivity. These alloys can be fabricated using casting and powder metallurgy techniques in which porosity is a common feature. The presences of pores adversely affect the mechanical properties and wear resistance of these components. Not only the total area percentage of porosity influences the degradation in properties but also size, shape and interconnectivity of pores play an important role. In this study, aluminum alloys were produced using powder metallurgy technique. The amount of porosity was varied by varying compaction pressure and amount of wax added before compaction. Reciprocating wear tests (ball-on-flat configuration) were performed against AISI 52100 bearing steel ball under both low (1.5-5N) and high (6-20N) loads. Scanning electron microscopy was employed in order to identify possible wear mechanisms. Both detrimental and beneficial effects of porosity under different loading conditions were observed. An attempt has been made to develop a relationship between pore size and distribution and wear behavior of aluminum alloys.

Publication History:
Received: August 29, 2015
Accepted: December 05, 2015
Published: December 08, 2015

Keywords:

Aluminum alloys, Powder Metallurgy, Porosity, Microstructure, wear

Introduction

Aluminum alloys are widely used in a variety of applications, including automotive, aerospace, air-conditioning equipment and home electrical appliances due to their high strength to weight ratio, high elastic modulus and good impact resistance [1-11]. However, low wear resistance compared to other materials (i.e. steels and ceramics), limits their use. The wear resistance of aluminum alloys depends on a number of microstructural parameters such as size, shape, natureand distribution of micro-constituents (porosity and second phase particles). The microstructural parameters are, to large extent, controlled by the particular manufacturing process employed [12-14].

Porosity is a common feature in all processing methods of Al alloys and strongly influences their properties and applications. It is a serious microstructural defect and has a negative impact on the mechanical properties of the alloy. The influence of porosity on the wear behavior of materials has been found to be rather complex and has not been clearly identified. It is pertinent to note that both beneficial and detrimental effects of porosity on wear resistance have been reported in the literature [15-17]. Chen et al. [18] investigated the influence of porosity on composite materials and suggested that porosity may help to absorb the impact energy that accompanies crack splitting. Simchi and Danninger [19] showed that porosity acts as lubricant reservoirs in wet sliding conditions, which provides a considerable advantage in wear process.

However, in general, the presence of porosity is accompanied by a decrease in mechanical properties, i.e., drop in strength and ductility of materials [20-32]. Hardin and Beckermann [33] demonstrated an apparent reduction in elastic moduli of components due to the presence of pores. Increase in porosity also decreases the fatigue strengths, hardness, facture toughness and elongation (%). Porosity appears to impact the process not merely by softening the material alone but also by promoting subsurface cracking and delamination. The emergence of stress concentrations around pores depend on pore size, shape and orientation, and leads to accelerated wear.Pores act as pre-existing incipient crack in the subsurface layer and becomes unstable at an appropriate stress level [34].The effect of pores on crack initiation and propagation under cyclic loading was investigated by many researchers. Suh [35] observed that an increase in porosity content reduces the required length of cracks needed to link up pores which promotes delamination. Gui et al. [36] considered the pores as crack sources which can be created when an external force is applied. At high porosity, materials have more interconnected pores, lower strength, and are much easier to deform and to be torn off. A decrease in pore density results in enhanced wear resistance since pores act as stress raisers and thus increase the probability of cracking and fracture. However, from fracture behavior point of view, pore size is more critical than the overall porosity content [25,26].

In addition, pore size is also important in terms of entrapping wear debris. In the case of specimens with low porosity and small mean pore size, the capture of debris by pores is difficult. Here, pores may be partially or completely closed by plastic deformation, decreasing the probability of pore filling by wear debris. In contrast, for high porosity levels and larger mean pore sizes, plastic deformation results in filling the pores with metallic particles. According to Dubrujeaud [17], the filling of pores with wear debris enhances wear resistance of materials by reinforcing the porous material. On the other hand, Deshpande and Lin [37] reported that porosity decreases wear resistance of material as a result of the no-load bearing characteristics of pores on the wear surface. Porosity increases surface roughness of materials, decreases the real area of contact between two sliding surfaces and consequently increases the contact pressure which promotes material removal during sliding [38].

In this study, in order to examine the effect of porosity on wear

***Corresponding Author:** Md. Aminul Islam, Department of Process Engineering and Applied Science, Materials Engineering Program, Dalhousie University, Halifax, Nova Scotia, B3J2X4, Canada; E-mail: md.aminul.islam@dal.ca

Citation: Sinha A, Islam MDA, Farhat Z (2015) Reciprocating Wear Behavior of Al Alloys: Effect of Porosity and Normal Load. Int J Metall Mater Eng 1: 117. doi: http://dx.doi.org/10.15344/2455-2372/2015/117

behavior of aluminum alloys, two manufacturing processes were employed to induce various pore sizes, shapes, distributions and amounts. Cold isostatic pressing and uniaxial compression were used, where the amount of porosity was varied by varying the amount of lubricant and compressive stress, respectively. Different manufacturing processes results in different amount, size and distribution of pores. Al 6061 and Al-6% Si were used in cold isostatic pressing and uniaxial compression, respectively. Reciprocating wear tests were performed at low and high normal loads in order to investigate the effect of normal load on wear. A relationship has been developed between pore size and distribution and wear behavior of aluminum alloys.

Experimental

Aluminum alloys were prepared using uniaxial compression and cold isostatic pressing (CIP). Al 6061and Al-6%Si alloys particle sizes are 71 µm and 55 µm respectively. During cold isostatic pressing, a total of 0%, 1.5%, 10.5% and 14.5% lubricant (Lico wax C) were added to the Al 6061 powder (97.5wt.% Al, 1wt.% Mg, 0.6wt.% Si, 0.5wt.% Fe, 0.1wt% Cu, 0.2wt.% Zn, 0.1 wt.% Mn) and blended in a Turbula Model T2M mixer for 40 minutes to ensure homogeneity. Rubber molds were filled with the blended powders andsealed with electrical tape. The sealed molds were then transferred to cold isostatic press (CIP) chamber. The chamber was filled with a mixture of water and water soluble oil (20:1). The pressure within the pressure chamber was increased to 200MPa by using a high pressure air-operated piston type pumpand maintained for a dwell time of 5 minutes. Using the decompression valve, the pressure was then reduced at a rate of 6.89 MPa.

During uniaxial compression, two powders (i.e., Al–Si and Al–Mg master alloys), were mixed to produce Al-6% Si alloy having following alloy composition; 88.8 wt.% Al, 6.0 wt.% Si, 4.5 wt.% Cu, 0.5 wt.% Zn and 0.2 wt.% Fe. A total of 1.5% Lico wax C was used as a pressing lubricant. Specimens were pressed at 100, 200 and 600 MPa and then sintered. Some of the specimens compacted at 600 MPa and sintered were swaged to reduce the amount of porosity further.All specimens (Al 6061 and Al-6% Si) were sintered in a tube furnace at 560°C for 20 minutes and then slow cooled to 480°C. Basic properties of the two alloys are given in Table 1.

Al 6061	Green density (g/cc)	Sintered density (g/cc)	Al-6%Si	Green density (g/cc)	Sintered density (g/cc)
0% wax	2.49	2.52	Pressed at 100 MPa	2.11	2.33
1.5% wax	2.24	2.32	Pressed at 200 MPa	2.29	2.46
10.5% wax	1.75	1.86	Pressed at 600 MPa	2.58	2.6
14.5% wax	1.48	1.57	Pressed at 600MPa and swaged	2.58	2.74

Table 1: Basic properties of Al 6061 and Al-6% Sialloy.

Dry reciprocating wear tests were performed using a Universal Micro-Tribometer. This test method utilizes a ball upper specimen that slides against a flat lower specimen in a linear, back and forth sliding motion having a stroke length of 5.03 mm. All tests were conducted at room temperature and at a relative humidity of 40–55 %. The load is applied downward through the ball counter-face against a flat specimen mounted on a reciprocating drive. The tester allows for monitoring the dynamic normal load and friction force during the test. A 6.3 mm diameter AISI 52100 bearing steel ball with a hardness of HRA 83 was used as a counter-face material. The ball was mounted inside a ball holder, which is attached directly to a suspension system. The suspension system is attached to a load sensor that controls and records forces during the test. The weight of the specimen was measured before and after each wear test to determine individual weight loss at selected time intervals. The operating conditions for reciprocating wear tests are given in Table 2. Specimens were cross-sectioned in order to observe the sub-surface of the wear track. Scanning electron microscopy was employed to identify possible wear mechanisms.

Test condition	Al 6061	Al-6%Si
Lubricant	None	None
Temperature	Ambient	Ambient
Pressure	1 atm	1 atm
Relative humidity	40-55%	40-55%
Stroke length	5.03 mm	5.03 mm
Load	1.5,2,2.5,3,4,5N	6,10,15,20N

Table 2: Operating conditions for reciprocating wear test.

Results and Discussion

Effect of lubricant content and compaction pressure on porosity

The size, shape, distribution and amount of pores in compacts are largely dependent on involved processing parameters, i.e. amount of lubricant and compaction pressure. For cold isostatic pressed (CIPed) specimens, surface porosity was varied by varying the amount of lubricant. Figure 1 shows the microstructures of CIPed specimens, where specimens were compacted and sintered under the same conditions and the amount of lubricant determines pore size, shape and amount. The surface porosity ranges from 3.5% to 20.7% for 0% lubricant to 14.5% lubricant, respectively. With increasing the lubricant content from 0% to 14.5%, not only the amount of porosity, but also pore size increased from 12µm to 33µm, while, the shape of pores changes from circular to irregular. However, the size and shape of aluminum grains remain constant. Aluminum grain size, pore size, volume and surface porosity for all lubricant contents are tabulated in Table 3.

Specimen	Wax (%)	Al grain size (µm)	Poresize (µm)	Volume porosity (%)	Surface porosity (%)
Al 6061	0	45.6	12.0	6.5	3.5
	1.5	46.1	20.0	13.8	10.3
	10.5	45.3	28.0	30.9	16.0
	14.5	45.7	33.0	41.7	20.7
Al-6%Si	Compaction Pressure	Al grain size (µm)	Pore size (µm)	Volume porosity (%)	Surface porosity (%)
	100 MPa	89.2	82.4	15.67	6.7
	200 MPa	99.6	70.2	10.50	4.2
	600 MPa	84.2	46.9	5.52	2.3
	Swaged	34.8	8.4	0.98	1

Table 3: Microstructural characteristics ofAl 6061 andAl-6%Si.

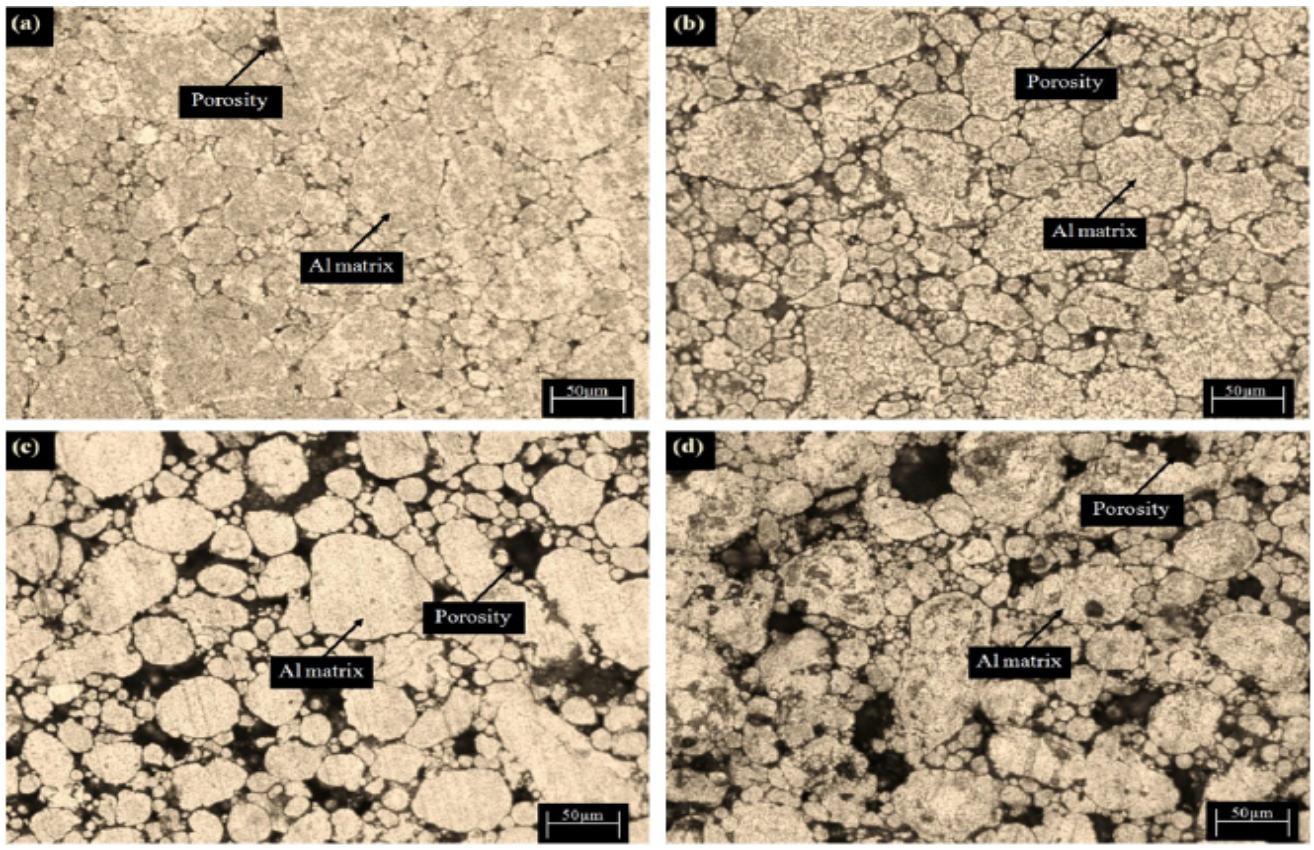

Figure1: Optical micrograph of Al 6061 samples with (a) 0% wax, (b) 1.5% wax, (c) 10.5% wax and (d) 14.5% wax content.

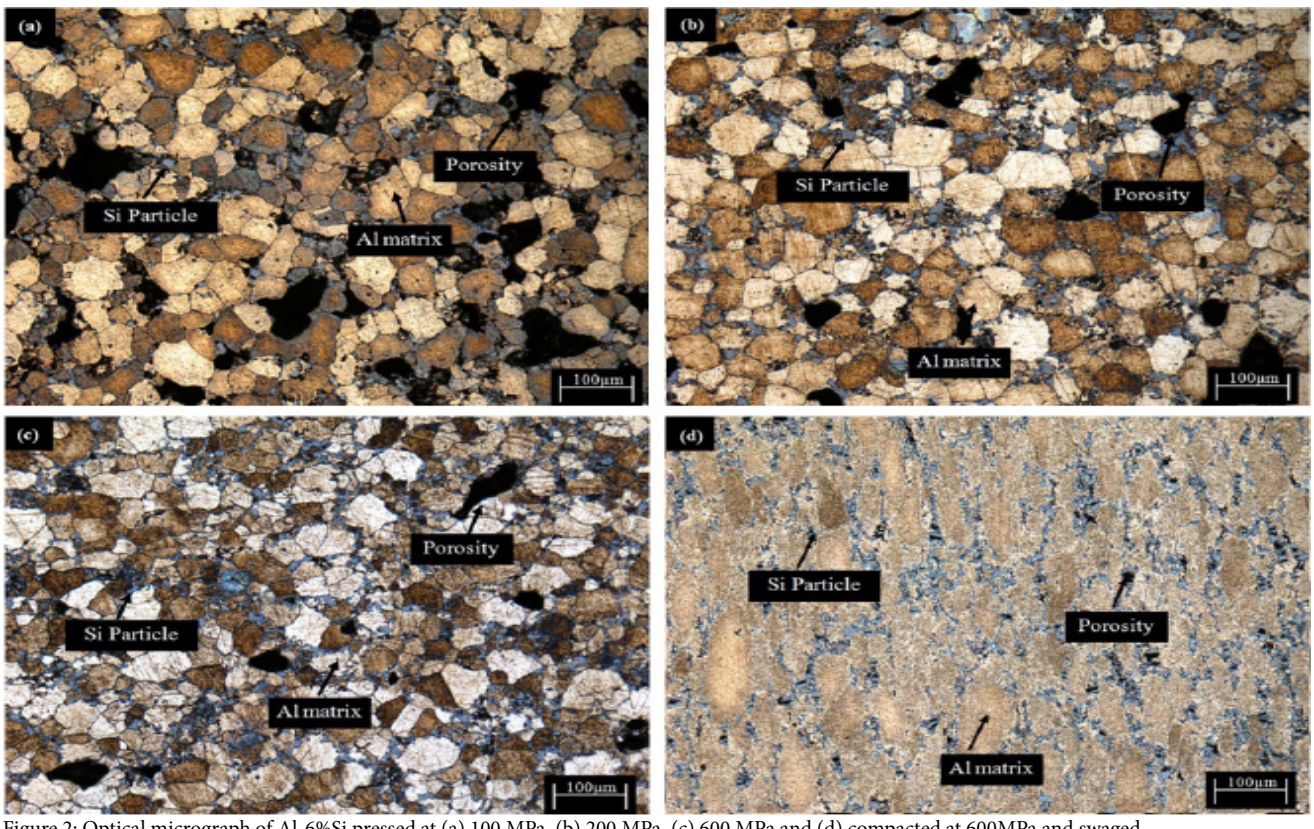

Figure 2: Optical micrograph of Al-6%Si pressed at (a) 100 MPa, (b) 200 MPa, (c) 600 MPa and (d) compacted at 600MPa and swaged.

For Al-6%Si alloy, both volume and surface porosity decrease with increasing compaction pressure (Figure 2). The volume percent porosity ranges from 5.52% for a 600MPa specimen to 15.67% for the 100MPa specimen, while surface porosities range from 2.3% to 6.7% for the same specimens, respectively. Higher compaction pressure leads to greater uniformity, lower porosity and enhanced density of the alloy.Al and Si grain sizes remain constant for 100MPa, 200MPa and 600MPa compaction pressure. Although the pores have irregular shape at low compaction pressure, they are uniformly distributed throughout the specimen.With increasing compaction pressure, pore shape changes from large irregular to a small round shape. However, the swaged specimens (Figure 2d) exhibit finer matrix and smaller Si particles. Table 3 shows the Al grain size, pore size, volume and surface porosity for all compacted specimens.

Figure 3 represents pore size for different lubricant content and compaction pressure. A linear increase in pore size was observed with increasing lubricant content. Here, the lubricant acts as a binding agent during the compaction process and goes in between the aluminum grains. During sintering, the lubricant burns off leaving behind pores in the material. Hence, higher amount of lubricant results in higher porosity and larger pore size. On the other hand, the pore size decreases with increasing the compaction pressure. Among all the specimens (both CIPed and uniaxially compacted), the largest pore size (82.4 μm) was observed at 100 MPa compaction pressure and the smallest pore size (8.4 μm) was observed for the swaged specimen.

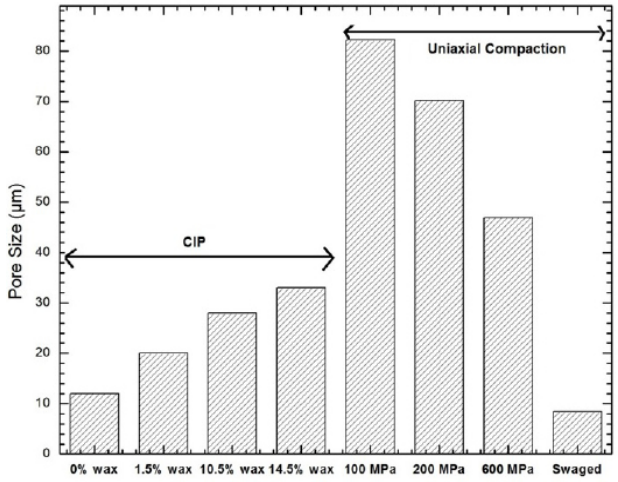

Figure 3: Dependence of average pore size on lubricant content and compaction pressure.

It is interesting to note that, there is around 6.4 fold increase in volume percent porosity with increasing the amount of lubricant to 14.5%, while only 2.75 fold increase in pore size was observed for same condition. Furthermore, there is around 15.9 fold decrease in volume and 9.8 fold decrease in pore size was observed for 100 MPa compacted specimen compared to swaged specimen. Specimens prepared through cold isostatic pressing have shown large range of porosity (in terms of volume and surface), hence, is used here to study the effect of pore distribution on wear resistance, while specimens prepared through uniaxial compression show larger range of pore size and it is used to study the effect of pore size on wear behavior.

Effect of porosity on hardness

In order to investigate the effect of porosity on the hardness of these alloys, a series of Rockwell hardness measurements were conducted. Figure 4 exhibits the variation of hardness with surface porosity for both Al 6061 and Al-6%Si specimens. The Rockwell hardness of Al 6061 containing 3.5%, 10.3%, 16.0% and 20.7% surface porosity are around 84, 67, 23 and 8 HRH, respectively. Here, 90% reduction in hardness is observed as porosity increases from 3.5% to 20.7%. This trend is in agreement with previous work [39].This is because, with increasing porosity, load bearing area decreases. Moreover, increased porosity in the subsurface raises the chances for crack nucleation and link-up of pores. This results in weakening of the materials and decreases strength.

Similarly, the hardness of Al-6%Si alloy doubles (Figure 4) as the surface porosity drops from 6.7% to 1%. The variation of hardness with porosity is expected to have a major impact on wear resistance.

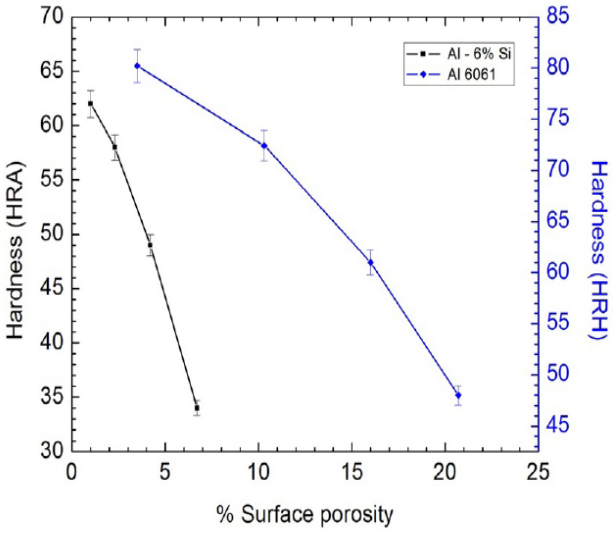

Figure 4: Variation in hardness with porosity content.

Wear behavior

Specimens containing different amounts of surface porosity were subjected to reciprocating wear tests. Figure 5 represents the weight loss vs sliding distance for CIPed specimens (Al 6061) containing 3.5% porosity. The plot reveals a somewhat linear increase in weight loss with sliding distance. Moreover, at any given sliding distance, weight loss increases with applied load. Similar trend is also observed for other conditions, which is in agreement with other researchers [40-52]. The wear rate was calculated from the slope of the weight loss versus sliding distance. In order to investigate the effect of porosity on wear resistance, wear rates of CIPed specimens (containing 3.5%, 10.3%, 16.0% and 20.7% surface porosity) are plotted as a function of normal load and surface porosity (Figure 6). It is evident from the figure that the wear rate increases with increasing surface porosity for all loading conditions. For example, at 2.5 N loads, there is around 2.5 fold increase in wear rate when surface porosity increased from 3.5% to 20.7%. Similar results (increase in wear rate with increasing porosity) were reported by other researchers [53,54]. Again, wear rate of the specimens increases with increasing normal load. There is around 2, 2.5, 2.2, and 1.5 fold increase in wear rate with increasing normal load from 1.5 N to 5 N for 3.5%, 10.3%, 16.0% and 20.7% surface porosity, respectively. This is because of the fact that, pores act as crack initiation site during wear. At low normal load, the pores beneath the worn surface remain stable due to small amount of subsurface deformation and strain. With increasing normal load, stress intensity increases. Pores beneath the worn surface become unstable and cracks originated from these pores can propagate significantly.

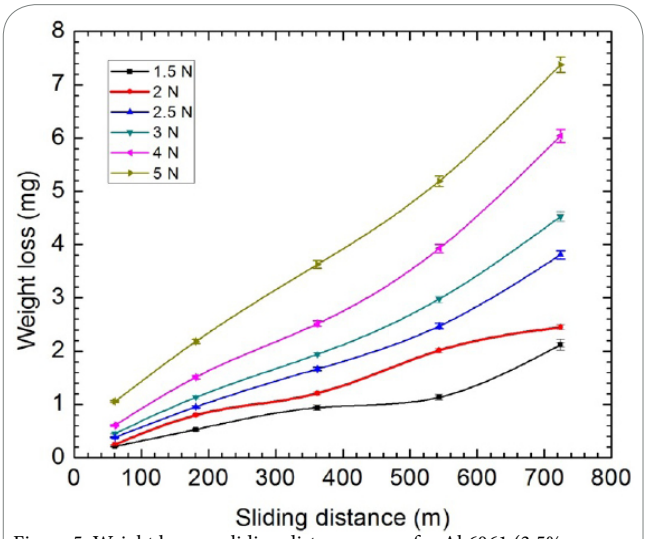

Figure 5: Weight loss vs. sliding distance curve for Al 6061 (3.5% porosity).

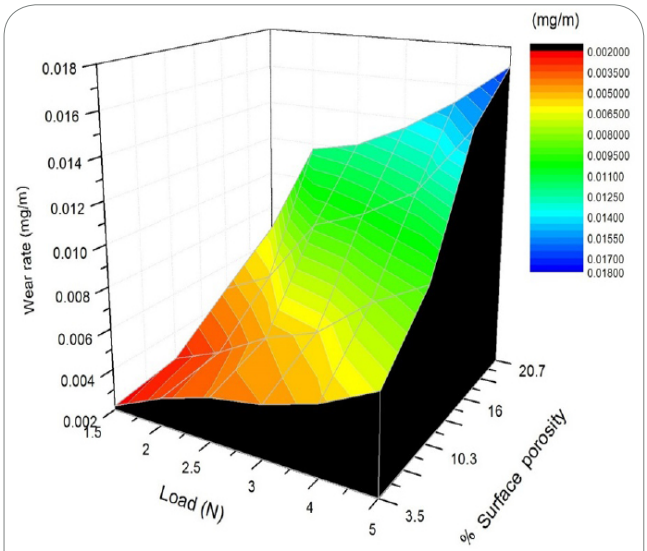

Figure 6: Variation of wear rate with normal load surface porosity for Al 6061.

As compaction pressure is decreased, % porosity increases which leads to lower hardness.The pore size increases and becomes more irregular in shape, consequently, wear rate increases (Figure 7). The increase in porosity resultsin more material removal by covering of pores and pore edge fracturing. Moreover, the chances of crack nucleation, and link-up of pores is increased with increasing porosity in the subsurface.Besides, the irregular shape of pores and increased pore sizes lead to higher probability of crack nucleation. As contact pressure is increased with increasing % porosity, wear rate drops. The increase in contact pressure is due to a pore-enhanced-surface-roughness of the specimens, which reduces the area of contact between the sliding pair. However, as % porosity increases over 4% due to lower compaction pressure, larger pores are formed and hardness drops; although, wear resistance increases (Figure 7). The effect of porosity on wear rate is not only due to softening but also pore size and when the pore size exceeds the contact area between the specimen and counter-face, wear rate drops. Hertzian contact analysis is carried out to identify possible factors which contribute to the wear rate of aluminum alloys. Based on the Hertzian theory, the contact radius 'a' can be determined from [55],

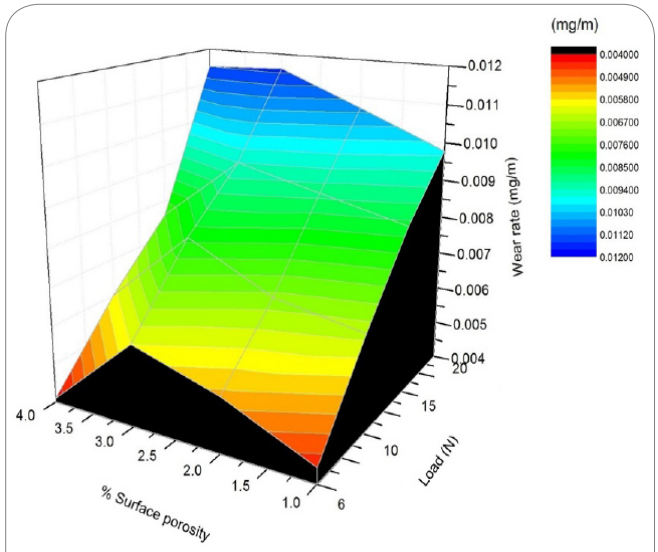

Figure 7: Variation of wear rate with normal load surface porosity for Al-6% Si.

$$a^3 = \frac{3WR}{4E^*}$$

where W is the total load on the contact spot and R is the effective radius which relates to the radius of the individual components by,

$$\frac{1}{R} = \frac{1}{R_1} + \frac{1}{R_2}$$

In the present work, all the samples are flat, which makes $R_2 = \infty$ and $R = R_1$. E^* is the effective modulus of elasticity:

$$\frac{1}{E^*} = \frac{1-\nu_1^2}{E_1} + \frac{1-\nu_1^2}{E_2}$$

E_1=210 GPa and E_2=90 GPa for the AISI 52100 steel ball and the Al-Si specimen, respectively. Here, ν_1 and ν_2 (both = 0.3) are Poisson's ratio of the specimen and the counter-face. For the low and the high loads of 6 N and 20 N, the contact radius is 0.05 and 0.08 mm, respectively. Hence, from the above analysis, the contact diameter in this load range varies from 0.10 to 0.16 mm which is in the same order of magnitude as the average pore size for the 100 MPa pressed and sintered specimen (pore size about 0.12 mm). This indicates that, the ball slides into the pore itself, which removes the contribution of pore covering and subsequent fracturing to material removal and wear occurs only by delamination. This eventually leads to lower wear.

Wear mechanisms

Worn surfaces were examined by using SEM to identify possible wear mechanisms. Abrasion, ploughing, delamination and heavy surface deformation and fracture are the dominant wear mechanisms during the wear process. Based on experimental observation, several factors are identified that affect the wear resistance of Al alloy, namely, the amount of porosity, pore size and shape.

Figure 8a shows heavy surface damage due to abrasion in the form of longitudinal grooves extending parallel to the sliding direction. This process of material removal from the surface via plastic deformation is known as ploughing [56-57]. During ploughing, material is deformed plastically, resulting in deepening and widening of wear tracks [58]. A series of grooves are formed due to the displacement of Al and ridges form along the sides of the ploughed grooves. These ridges become

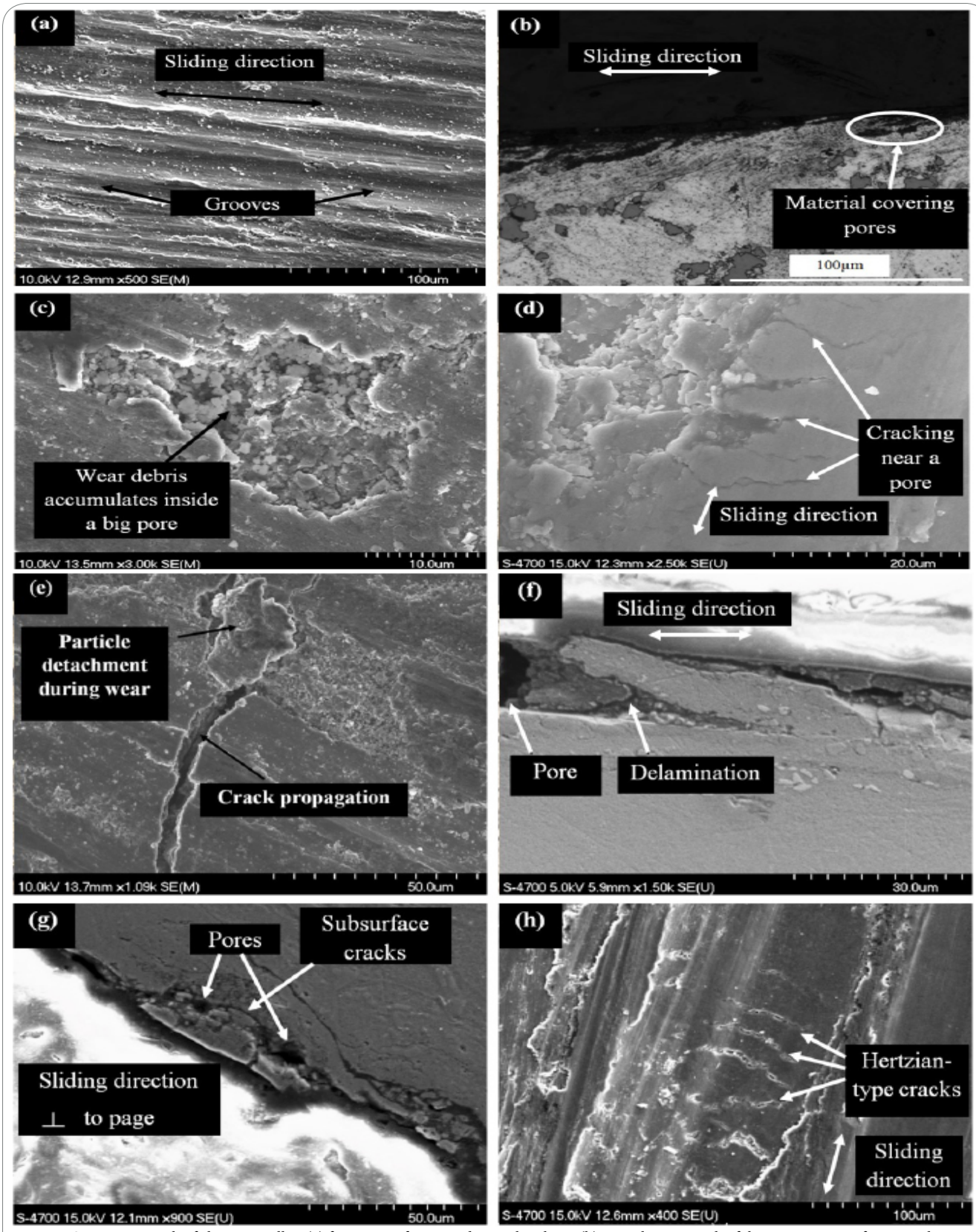

Figure 8: SEM micrograph of aluminum alloy, (a) formation of grooves due to ploughing, (b) optical micrograph of the cross-section of wear track shows pore covering by deformed material, (c) entrapments of wear debris inside a pore, (d) crack initiation near a pore, (e) crack propagation, (f) cross section of the wear track illustrating delamination, (g) cross section of the wear track showing the propagation of sub-surface crack due to the presence of porosity and (h) Hertzian-type cracks developed due to surface tensile stress.

flattened and eventually fracture after repeated loading and unloading cycles. Figure 8b is an optical micrograph of 600 MPa pressed and sintered Al-Si specimen at the end of the reciprocating wear test. The image represents a transverse cross section of the wear track (along the wear track). The figure shows material extending and partially covering pore cavity with a thin layer of deformed metal. The formation of the extruded metal over the pores occurs as a result of asperities ploughing through the surface and dragging material ahead of the slider. The extended material fractures and forms wear debris during subsequent passes of the slider. In some cases, some of the debris was entrapped into the pores (Figure 8c) and some were remained on top of the sliding surfaces causes three body abrasion. Again, as pores act as stress concentration areas they tend to fracture with the reciprocating motion of the slider. This is evident from the cracks extending from pore edges in Figure8d. Figure 8e shows a magnified image illustrating the crack initiation and propagation due to the reciprocation motion, where the pore is covered by the wear fragment.

Another mechanism which contributes to the observed wear is delamination. Delamination wear occurs as a result of subsurface cracks nucleation near pores (as they act as stress concentration regions) and propagation of these cracks (Figure 8f). There is a critical crack length beyond which it becomes unstable and propagates to the surface generating wear debris. Networks of cracks are created by connecting different subsurface pores (Figure 8g). Pores serve as the origin of crack generation and the end of crack propagation, hence, reducing the required length for crack propagation. Other wear features have been identified in all specimens are Hertzian cracks perpendicular to the sliding direction (Figure 8h). These cracks develop as a result of surface tensile stresses that develop during Hertzian contact.

The effect of porosity on wear resistance depends not only on the total porosity content, but also on pore distribution and connectivity of the pores. Figure 9 shows a schematic diagram illustrating the effect of pore distribution on wear. When the amount of porosity is small and pores are non-uniformly distributed (Figure 9a), it is difficult for the nucleated crack to propagate and connect with the adjacent pores. However, with increasing the amount of porosity and uniformly distributed pores, cracks can propagate at higher rate as pores can easily link up with each other and form a large network of cracks. This is because, the distance cracks needed to travel before meeting another pore is shorter, which significantly increases wear rate.

Figure 10 is a schematic diagram which depicts the effect of pore size on wear mechanisms. Figure 10(a-c) represents the covering of a small pore by extruded material ahead of the sliding counter-face and subsequent fracturing due to the further passes of the slider. Figure 10(d-f) illustrates the counter-face sliding inside a large pore, where the pore size and the contact area are within the same order of magnitude. This model further explains the drop in wear rate at both high porosity and large pore size for Al-6% Si. Dubrujeaud et al. [17] reached at similar conclusions that high porosity and large pore size have a beneficial effect on wear rate. However, they concluded that the drop in wear rate at high porosity content is attributed to the entrapment of wear debris in large pores.

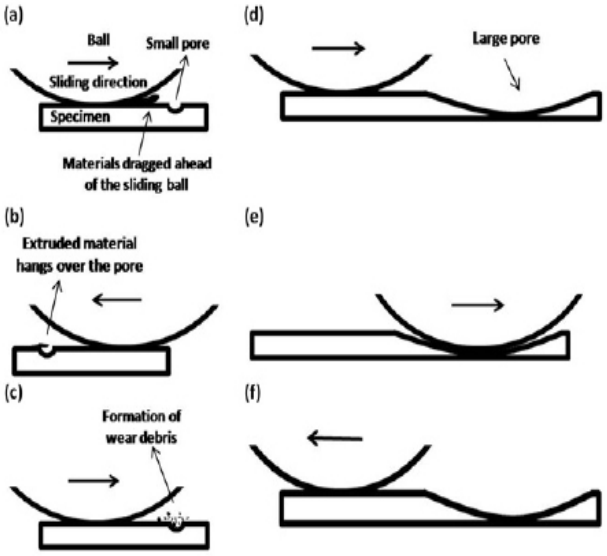

Figure 10: Schematic diagram depicting wear mechanisms observed for small and large pores.

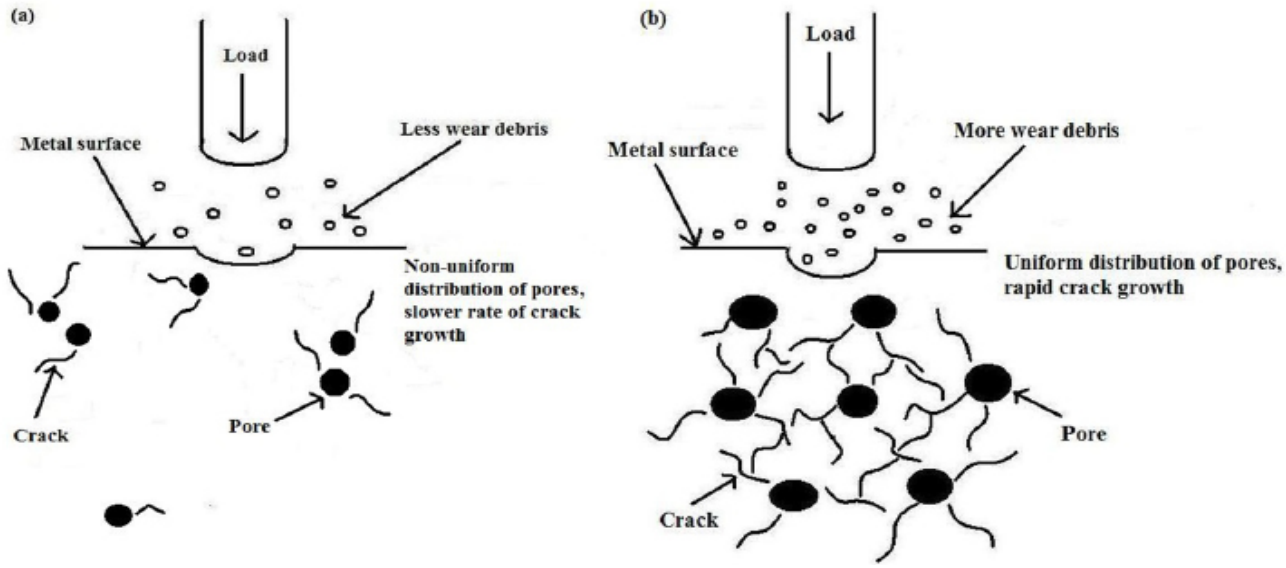

Figure 9: Schematic diagram depicting the effect of (a) non-uniform and (b) uniform pore distribution on wear.

Conclusion

In this study tribological behavior of Al alloys has been investigated. Specimens were prepared using cold isostatic pressing and uniaxial compression. The following main conclusions have emerged:

1. There is an inverse relationship exists between the hardness and porosity content of Al alloys. Significant decrease in hardness was observed with an increase in surface porosity.

2. Wear rate of aluminum alloys increases with increasing normal load due to high contact pressure and heavy plastic deformation. Above a threshold normal load, porosity in the sub-surface region acts as a crack initiation site and promotes delamination.

3. The amount of porosity, distribution, size and shape of the pores has a great impact on material removal during wear. In general, the wear rate of Al alloy decreases with increasing porosity and for a given amount of porosity, uniform pore distribution results in accelerated wear.

4. Below a certain critical pore size, wear occurs by two mechanisms: (i) partial covering of pores with a thin layer of deformed material and break-up on subsequent passes of the slider; (ii) nucleation of cracks at subsurface pores and connecting to other pores, this ultimately lead to delamination of wear particles.

5. When pore size is in the same order of magnitude as the contact area between the counter-face and the specimen, the counter-face slides in to the pores, hence, pores become less effective in generating wear debris.

6. Abrasion, ploughing, delamination, heavy surface deformation and fracture are identified as the operative wear mechanisms during the wear process.

Competing Interests

The authors have no competing interests with the work presented in this manuscript.

Author Contributions

All the authors substantially contributed to the study conception and design as well as the acquisition and interpretation of the data and drafting the manuscript.

Funding

The authors acknowledge the financial support provided by Auto21 and Mr. Randy Cooke for his assistance in sample preparation.

References

1. Sarkar AD, Clarke J (1980) Friction and Wear of Aluminum-Silicon alloys. Wear 61:157-167.
2. Sarkar AD (1975) Wear of Aluminum-Silicon Alloys. Wear 31: 331-343.
3. Torabian H, Pathak JP, Tiwari SN (1994) Wear Characteristics of Al-Si Alloys. Wear 171: 49-58.
4. Hanna AH, Shehata F (1992) Friction and Wear of Al-Si Alloys. Lubrication Engineering 49: 473-476.
5. Konishi T, Klaus EE, Duda JL (1995) Wear Characteristics of Aluminum-Silicon Alloy Under Lubricated Sliding Conditions. SILE Preprint No. 95-MP-5E-1, 50th Annual Meeting of SILE, Chicago, Illinois, May 14-19.
6. Davis FA, Eyre TS (1994) The Effect of silicon Content and Morphology on the Wear of Aluminum-Silicon Alloys Under Dry and Lubricated Sliding Conditions. Tribology International 27: 171-181.
7. Barber GC, Matthews JJ, Jafry S (1991) Wear and Scuff Resistance of Aluminum 390. Lubrication Engineering 47: 423-430.
8. Ferrante J, Brainard WA (1979) Wear of Aluminum and Hypoeutectic Aluminum-Silicon Alloys in Boundary Lubricated Pin-on-Disk Sliding. NASA Technical Paper 1442.
9. Wang HW, Skeldon P, Thompson GE (1999) Tribological Enhancement of Aluminium by Porous Anodic Films Containing Solid Lubricants of MoS2 Precursors. Tribology Transactions 42: 202-209.
10. Goto, H., Omori, S. (2000) Tribological Characteristics of Particle and Chopped Fiber-Reinforced Al-Si Alloy Matrix Composites. Tribology Transactions 43: 57-65.
11. Rameshkumar T, Rajendran I (2013) Mechanical and Tribological Properties on Al-Sn-Si Alloy-Based Plain Bearing Material. Tribology Transactions 56: 268-274.
12. Prasad BK, venkateswarlu K, Modi OP, Jha AK, Das S, et al. (1998) Sliding Wear Behavior of some Al-Si Alloys: Role of shape and size of Si particles and Test conditions. Metallurgical and Materials Transactions 29A: 2747-2752.
13. Shivanath R, Sengupta PK, Eyre TS (1997) Wear of Aluminium-Silicon Alloys. The British Foundrymen 70: 349-356.
14. Yassen RS, Dwarakadasa ES (1983) Wear of Aluminium under Dry Sliding Conditions. Wear 84: 375-379.
15. Proudhon H, Savkova J, Basseville S, Guipont V, Jeandin M, et al. (2014) Experimental and numerical wear studies of porous Reactive Plasma Sprayed Ti-6Al-4V/TiN composite coating. Wear 311: 159-166.
16. Lin Z, hui QX, Bo-hua D, Xin-Bo H, Ming-li Q (2008) Effect of porosity on wear resistance of SiCp/Cu composites prepared by pressureless infiltration. Transactions of Nonferrous Metal Society of China 18:1076-1082.
17. Dubrujeaud B, Vardavoulias M, Jeandin M (1994) The role of porosity in the dry sliding wear of a sintered ferrous alloy.Wear 174: 155-161.
18. Chen Q, Li D, Cook B (2009) Is porosity always detrimental to the wear resistance of materials? A computational study on the effect of porosity on erosive wear of TiC/Cu composites. Wear 267: 1153-1159.
19. Simchi A, Danninger H (2004) Effects of porosity on delamination wear behaviour of sintered plain iron. Powder Metallurgy 47: 73-80.
20. Li DY, Luo YC (2001) Effects of TiN nano-particles on porosity and wear behavior of TiC/TiNi tribo composite. Journal of Materials Science Letters 20: 2249-2252.
21. Hamid AA, Ghosh P, Jain S, Ray S (2006) Influence of particle content and porosity on the wear behaviour of cast in situ Al(Mn)–Al2O3(MnO2) composite. Wear 260: 368-378.
22. Sarikaya O (2005) Effect of some parameters on microstructure and hardness of alumina coatings prepared by the air plasma spraying process. Surface& Coatings Technology 190: 388- 393.
23. Raghukiran N, Kumar R (2013) Processing and dry sliding wear performance of spray deposited hyper-eutectic aluminum–silicon alloys. Journal of Materials Processing Technology 213: 401- 410.
24. Kanchanomaia C, Saengwichian B, Manonukul A (2013) Delamination wear of metal injection moulded 316L stainless steel. Wear 267: 1665-1672.
25. Tekmen C, Ozdemir I, Cocen U, Onel K (2003) The mechanical response of Al–Si–Mg/SiCp composite: influence of porosity. Materials Science and Engineering A 360: 365-371.
26. Danninge H, Jangg G, Weiss B, Stickler R (1993) Microstructure and mechanical properties of sintered iron. Part I. Basic considerations and review of literature. Powder Metallurgy International 25: 111-117.
27. Bergmark A, Alzati L, Persson U (2002) Crack initiation and crack propagation in copper powder mixed PM steel. Powder Metallurgy Progress 2: 222-230.
28. Gerard DA, Koss DA (1990) Low cycle fatigue crack initiation: modeling the effect of porosity. International. Journal of Powder Metallurgy 26: 337-343.
29. Sahin Y (2003) Preparation and some properties of SiC particle reinforced aluminium alloy composites. Materials and Design 24: 671-679.
30. Sahin Y, Acilar M (2003) Production and properties of SiCp-reinforced aluminium alloy composites. Composites: Part A Applied Science and Manufacturing 34: 709-718.
31. Yih P, Chung DDL (1997) Titanium diboride copper-matrix composites. Journal of Materials Science 32: 1703-1709.

32. Lu Y, Liu Z (2013) Coupled Effects of Fractal Roughness and Self-Lubricating Composite Porosity on Lubrication and Wear. Tribology Transactions 56: 581-591.

33. Hardin RA, Beckermann C (2007) Effect of porosity on the stiffness of cast steel. Metallurgical And Materials Transactions A 12: 2992-3006.

34. Ray S, Fishman SG, Dhingra AK (1988) Proceedings on Cast Reinforced Metal Composites. ASM International 77-86.

35. Suh NP (1977) An overview of the delamination theory of wear. Wear 44: 1-16.

36. Gui M, Kang, SB Lee, JM (2000) Influence of porosity on dry sliding wear behaviour in spray deposited Al-6Cu-Mn/SiCp composite. Materials Science and Engineering A 293: 146-56.

37. Deshpande PK, Lin RY (2006) Wear resistance of WC particle reinforced copper matrix composites and the effect of porosity. Materials Science and Engineering A 418: 137-145.

38. Vardavoulias M, Jouanny-Tresy C, Jeandin M (1993) Sliding-wear behaviour of ceramic particle-reinforced high-speed steel obtained by powder metallurgy. Wear 165: 141-149.

39. Islam MDA, Farhat ZN (2011) Effect of porosity on dry sliding wear of Al–Si alloys. Tribology International 44: 498-504.

40. Dwivedi DK (2010) Adhesive wear behaviour of cast aluminium–silicon alloys: Overview. Materials and Design 31: 2517-2531.

41. Elmadagli M, Perry T, Alpas AT (2007) A parametric study of the relationship between microstructure and wear resistance of Al–Si alloys. Wear 262: 79-92.

42. Singla M, Singh L, Chawla V (2009) Study of Wear Properties of Al-SiC Composites. Journal of Minerals & Materials Characterization & Engineering 8: 813-819.

43. Wei MX, Chen KM, Wang SQ, Cui XH (2011) Analysis for Wear Behaviors of Oxidative Wear. Tribology Letters 42:1-7.

44. Kumar S, Balasubramanian V (2010) Effect of reinforcement size and volume fraction on the abrasive wear behaviour of AA7075 Al/SiCp P/M composites-A statistical analysis. Tribology International 43: 414-422.

45. Corrochanoa J, Walker JC, Lieblich M, Ibanez J, Rainforth WM (2011) Dry sliding wear behaviour of powder metallurgy Al–Mg–Si alloy-MoSi2 composites and the relationship with the microstructure.Wear 270: 658-665.

46. Bermudez MD, Martinez-Nicolas G, Carrion FJ, Martinez-Mateo I, Rodriguez JA, et al. (2001) Dry and lubricated wear resistance of mechanically-alloyed aluminium-base sintered composites. Wear 248: 178–186.

47. Yasmin T, Khalid AA, Haque MM (2004) Tribological (wear) properties of aluminum–silicon eutectic base alloy under dry sliding condition. Journal of Materials Processing Technology 153–154: 833-838.

48. Hamn MD, Talib LA, Daud AR (1996) Effect of element additions on wear property of eutectic aluminium-silicon alloys.Wear 194: 54-59.

49. Casellas D, Beltran A, Prado JM, Larson A, Romero A (2004) Microstructural effects on the dry wear resistance of powder metallurgy Al–Si alloys. Wear 257:730-739.

50. Mohammad ES, Karimzadeh F (2011) Wear behavior of aluminum matrix hybrid nanocomposites fabricated by powder metallurgy. Wear 271: 1072–1079.

51. Rahimian M, Parvin N, Ehsani N (2011) The effect of production parameters on microstructure and wear resistance of powder metallurgy Al–Al2O3 composite. Materials and Design 32:1031–1038.

52. Ravindran P, Manisekar K, Rathika P, Narayanasamy P (2013) Tribological properties of powder metallurgy Processed aluminium self lubricating hybrid composites with SiC additions. Materials and Design 45: 561-570.

53. Hamid AA, Ghosh PK, Jain SC, Ray S (2008) The influence of porosity and particles content on dry sliding wear of cast in situ Al(Ti)–Al2O3(TiO2) composite. Wear 265: 14–26.

54. Yılmaz O, Buytoz S (2001) Abrasive wear of Al2O3-reinforced aluminium-based MMCs. Composites Science and Technology 61: 2381-2392.

55. Johnson K (1987) Contact mechanics, Cambridge University Press, UK.

56. Gyimah GK, Chen D, Huang P (2008) Dry Sliding Studies of Porosity on Sintered Cu-based Brake Materials. Transaction on control and mechanical systems 2: 219-224.

57. Alshmri F, Atkinson HV, Hainsworth SV, Haidon C, Lawes SDA (2014) Dry sliding wear of aluminium-high silicon hypereutectic alloys. Wear 313: 106-116.

58. Deya SK, Perry TA, Alpas AT (2009) Micromechanisms of low load wear in an Al-18.5% Si alloy. Wear 267: 515-524.